

Quantum-control approach to realizing a Toffoli gate in circuit QED

Vladimir M. Stojanović,¹ A. Fedorov,² A. Wallraff,² and C. Bruder¹

¹*Department of Physics, University of Basel, Klingelbergstrasse 82, CH-4056 Basel, Switzerland*

²*Department of Physics, ETH Zürich, CH-8093 Zürich, Switzerland*

(Dated: February 18, 2022)

We study the realization of a Toffoli gate with superconducting qubits in a circuit-QED setup using quantum-control methods. Starting with optimized piecewise-constant control fields acting on all qubits and typical strengths of XY -type coupling between the qubits, we demonstrate that the optimal gate fidelities are affected only slightly by a “low-pass” filtering of these fields with the typical cutoff frequencies of microwave driving. Restricting ourselves to the range of control-field amplitudes for which the leakage to the non-computational states of a physical qubit is heavily suppressed, we theoretically predict that in the absence of decoherence and leakage, within 75 ns a Toffoli gate can be realized with intrinsic fidelities higher than 90%, while fidelities above 99% can be reached in about 140 ns.

PACS numbers: 03.67.Lx, 03.67.Ac

Superconducting (SC) qubits [1] have come a long way since the realization that Josephson physics in SC circuits can be utilized to prepare well-defined few-level quantum systems [2]. Coupling such qubits is essential for quantum computation. The most successful approaches up to now rely on coupling all the qubits in an array to an “interaction bus,” a central coupling element having the form of a transmission line with electromagnetic modes. In the circuit quantum electrodynamics (circuit QED) regime strong coupling between the qubits and the confined photons is realized [3–5]; the cavity photons induce a long-range coupling between the qubits. The combination of transmon qubits [6] and co-planar microwave cavities represents the state-of-the-art of microwave quantum optics.

The environmental degrees of freedom limit the time over which quantum coherence can be preserved. While they are similar to charge qubits, transmons have a much larger total capacitance such that the charging energy is significantly smaller than the Josephson energy. A small charge dispersion of the energy eigenstates leads to a reduced sensitivity to charge noise and longer dephasing times (T_2) [6]. Recently, a significant progress has been achieved [7, 8], with T_2 times being increased by an order of magnitude from $T_2 \sim 1 \mu\text{s}$ to $T_2 \sim 20 \mu\text{s}$.

Given that two-qubit gates with SC qubits have been demonstrated with fidelities higher than 90% [9], a key challenge now is to realize three-qubit ones with shortest possible gate times. An example is the Toffoli gate (controlled-controlled-NOT), which is relevant for quantum-error correction [10] and has already been implemented with trapped ions [11] and photonic systems [12] with respective fidelities of 71% and 81%. Very recently, several groups realized a Toffoli gate using superconducting circuits [13–15]. The Toffoli gate was implemented by a sequence of single- and two-qubit gates (direct approach).

In this paper, we adopt an alternative approach and

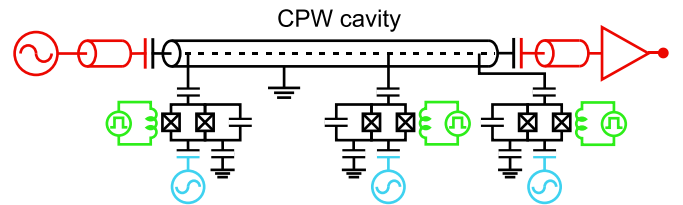


FIG. 1: Lumped-element circuit diagram of three transmon qubits coupled to a superconducting transmission-line resonator. The resonator serves as a coupling bus for the qubits and is also used for the readout of their states (red). Local flux lines (blue) allow for individual control of the qubit frequencies on the nanosecond time-scale. Microwave lines (green) are used to create control fields, each acting on its corresponding qubit.

study the realization of a Toffoli gate with SC qubits in a circuit-QED setup (for an illustration, see Fig. 1) by applying quantum-control methods [16] to the effective XY -type Hamiltonian of an interacting three-qubit array. We do so for realistic qubit-qubit coupling strengths and under typical experimental constraints on the qubit decoherence times.

We first determine optimal piecewise-constant control fields and evaluate the resulting gate fidelities. Then we discuss how these fidelities are affected when the control pulses are smoothed by eliminating their high-frequency Fourier components (spectral “low-pass” filtering). Our most important theoretical prediction is that within 75 ns a Toffoli gate can be realized with intrinsic fidelities (in the absence of decoherence and leakage) higher than 90%, while fidelities higher than 99% can be obtained in approximately 140 ns.

Methods of quantum control [16] have been put forward in a number of theoretical proposals for realizing quantum logic gates with SC qubits [17–19], thus complementing studies that solely involve time-independent Hamiltonians [20]. More fundamentally, recent studies

in operator (state independent) control [21] have been focusing on interacting systems and employing the concept of local control [22, 23]. The essential idea is that systems such as coupled spin-1/2 chains, models of interacting qubit arrays, can often be controlled by acting on a small subsystem. For instance, controlling only one end spin of an XXZ -Heisenberg chain ensures complete controllability of the chain [22, 23]. Yet, in view of the currently available few-qubit experimental setups [24], more important than restricting control to only one qubit is to be able to carry out an optimal control-pulse sequence within times much shorter than T_2 . This is necessary in order to minimize the undesired decoherence effects [1].

Under the condition of resonant driving and assuming that the qubits are in resonance with one another, the effective (time-independent) XY -type (flip-flop) qubit-qubit interaction Hamiltonian is given by

$$H_0 = \sum_{i < j} J_{ij} (\sigma_{ix} \sigma_{jx} + \sigma_{iy} \sigma_{jy}), \quad (1)$$

where σ_{ix} , σ_{iy} , and σ_{iz} are the Pauli matrices. The system is acted upon by time-dependent Zeeman-like control fields described by the Hamiltonian

$$H_c(t) = \sum_{i=1}^3 \left[\Omega_x^{(i)}(t) \sigma_{ix} + \Omega_y^{(i)}(t) \sigma_{iy} \right], \quad (2)$$

thus the system dynamics is governed by the total Hamiltonian $H(t) = H_0 + H_c(t)$.

The control fields $\Omega_x^{(i)}(t)$ and $\Omega_y^{(i)}(t)$ can be implemented using arbitrary wave generators (recall Fig. 1), which can produce an arbitrary signal with frequencies up to 500 MHz with minor distortions. In qubits based on weakly-anharmonic oscillators, leakage from the two-dimensional qubit Hilbert space (computational states) is the leading source of errors at short gate times [19, 26]. This is especially pronounced if the control bandwidth is comparable to the anharmonicity [18]. We therefore impose an additional constraint on the control fields, viz. the condition that

$$\Omega_{\max} = \max_{i,t} \sqrt{[\Omega_x^{(i)}(t)]^2 + [\Omega_y^{(i)}(t)]^2} \quad (3)$$

is smaller than some threshold value for the transmon to be a well-defined two-level system. For typical anharmonicities of transmon qubits (300 – 400 MHz) and values of Ω_{\max} of 100 – 130 MHz the error associated with this leakage should not exceed a few percent. While control schemes explicitly involving the higher levels of a physical qubit are in principle conceivable, in the present study we aim for simplicity and will in the following determine the control pulses for a system of qubits that are genuine two-level systems.

Before evaluating numerically the optimal control pulses we would like to comment on the controllability

aspects of the problem. Using the standard algorithm (see, for example, Ref. 16), it is straightforward to check that the dynamical Lie algebra of the system, generated by the skew-Hermitian operators $-iH_0$, $-i\sigma_{ix}$, and $-i\sigma_{iy}$ ($i = 1, 2, 3$), has dimension $63 = d^2 - 1$ ($d = 8$ is the dimension of the Hilbert space of the system). This Lie algebra is isomorphic to $su(d = 8)$ and the system is completely (operator) controllable. An arbitrary quantum gate can thus in principle be realized using properly designed control fields.

Our goal is to find the time dependence of control fields $\Omega_x^{(i)}(t)$ and $\Omega_y^{(i)}(t)$ for realizing a quantum Toffoli gate. We start our analysis with simple piecewise-constant control fields [23] acting on all three qubits in alternation in the x - and y directions with control amplitudes $\Omega_{x,n}^{(i)}$ and $\Omega_{y,n}^{(i)}$ ($n = 1, \dots, N_t/2$; $i = 1, 2, 3$).

At $t = 0$ control pulses are applied in the x direction to all three qubits with constant amplitudes $\Omega_{x,1}^{(i)}$ during the time interval $0 \leq t \leq T$. The Hamiltonian of the system is then $H_{x,1} \equiv H_0 + \sum_{i=1}^3 \Omega_{x,1}^{(i)} \sigma_{ix}$. Then y control pulses with amplitudes $\Omega_{y,1}^{(i)}$ are applied during the interval $T \leq t \leq 2T$, whereby the system dynamics is governed by $H_{y,1} \equiv H_0 + \sum_{i=1}^3 \Omega_{y,1}^{(i)} \sigma_{iy}$. This sequence of alternating x and y control pulses is repeated until N_t pulses have been completed at the gate time $t_g \equiv N_t T$. The time-evolution operator $U(t = t_g)$ is then obtained as a product of the consecutive $U_{x,n} \equiv \exp(-iH_{x,n}T)$ and $U_{y,n} \equiv \exp(-iH_{y,n}T)$, where $n = 1, \dots, N_t/2$.

For varying choices of N_t and T , the $3N_t$ control amplitudes are determined so as to maximize the fidelity

$$F(t_g) = \frac{1}{8} \left| \text{tr} [U^\dagger(t_g) U_{\text{TOFF}}] \right|, \quad (4)$$

where U_{TOFF} is the Toffoli gate. The numerical maximization over these amplitudes is carried out using the Broyden-Fletcher-Goldfarb-Shanno (BFGS) algorithm [27], a standard second-order quasi-Newton-type procedure. Based on an initial guess for the control amplitudes, the algorithm generates iteratively new sequences of amplitudes such that in each iteration step the fidelity is increased, terminating when the desired accuracy is reached. This procedure is repeated for multiple (~ 200) initial guesses to avoid getting trapped in local (instead of the global) maxima of $F(t_g)$. The optimization is performed under the constraint $\Omega_{\max} < 130$ MHz.

While piecewise-constant control pulses are convenient as a starting point for a theoretical analysis, the actual pulse-shaping hardware cannot generate such fields with arbitrarily-high frequency components. Turning the time course of piecewise-constant control pulses into an optimized shape can be considered the central problem of numerical optimal control [28].

We therefore perform spectral filtering of our optimal control fields. Quite generally, after acting with a frequency-filter function $f(\omega)$ on the Fourier transforms

$\mathcal{F}[\Omega_j^{(i)}(t)]$ of the optimal fields $\Omega_j^{(i)}(t)$ ($j = x, y$), one switches back to the time domain via inverse Fourier transformation to obtain the filtered fields $\tilde{\Omega}_j(t)$:

$$\tilde{\Omega}_j^{(i)}(t) = \mathcal{F}^{-1}[f(\omega)\mathcal{F}[\Omega_j^{(i)}(t)]] \quad (j = x, y). \quad (5)$$

In particular, we consider an *ideal low-pass* filter, which removes frequencies above the cut-off ω_0 and below $-\omega_0$. In other words, $f(\omega) = \theta(\omega + \omega_0) - \theta(\omega - \omega_0)$, where $\theta(x)$ is the Heaviside function. When applied to our piecewise-constant control fields, the transformations in Eq. (5) can be carried out semi-analytically. They lead to

$$\begin{aligned} \tilde{\Omega}_x^{(i)}(t) &= \frac{1}{\pi} \sum_{n=1}^{N_t/2} \Omega_{x,n}^{(i)} [a_{2n-1}(t) - a_{2n-2}(t)], \\ \tilde{\Omega}_y^{(i)}(t) &= \frac{1}{\pi} \sum_{n=1}^{N_t/2} \Omega_{y,n}^{(i)} [a_{2n}(t) - a_{2n-1}(t)], \end{aligned} \quad (6)$$

where $a_m(t) \equiv \text{Si}[\omega_0(mT - t)]$ ($m \in \mathbb{N}$) and $\text{Si}(x) \equiv \int_0^x (\sin t/t) dt$ stands for the sine integral. Based on Eq. (6), we numerically determine the time-evolution operators corresponding to the filtered control fields using a product-formula approach (for details, see the Appendix in Ref. 23). We then obtain the fidelities $\tilde{F}(t_g)$ corresponding to the filtered fields from an analog of Eq. (4).

Our numerical results are summarized in Table I. It shows examples of calculated Toffoli-gate fidelities for optimal piecewise-constant control fields (F) and their low-pass filtered versions (\tilde{F}), for two different high-frequency cutoffs ($\omega_0 = 500$ MHz and $\omega_0 = 450$ MHz). The last column of the table shows the maximum $\tilde{\Omega}_{\max}$ of $\sqrt{[\tilde{\Omega}_x^{(i)}(t)]^2 + [\tilde{\Omega}_y^{(i)}(t)]^2}$ over all qubits and all times and obeys the constraint discussed after Eq. (3). The fidelities corresponding to the piecewise-constant fields are virtually unaffected by the filtering process, since the highest frequencies achievable by current pulse-shaping hardware are much larger than the qubit-qubit coupling strengths.

To make contact with possible experiments, we now assume $J = 30$ MHz and $J_{12} = J_{23} = 6J_{13} = J$ [25]. As can be inferred from the table, a Toffoli gate can be realized in $2.25J^{-1} = 75$ ns with a fidelity higher than 90%, while fidelities larger than 99% can be reached for gate times of around $4.18J^{-1} = 140$ ns. Examples of optimal x and y control fields on all three qubits are shown in Fig. 2.

For fixed total time $t_g = N_t T$ higher fidelities are obtained for larger N_t (i.e., smaller T), and the same is true of the robustness of these fidelities to random errors in the control-field amplitudes [23]. However, for T smaller than some (nonuniversal) threshold value, it becomes impossible to reach high fidelities ($F > 90\%$) without violating the constraint $\tilde{\Omega}_{\max} < 130$ MHz.

TABLE I: Examples of calculated intrinsic Toffoli-gate fidelities for optimal piecewise-constant control fields (F) and their low-pass filtered versions (\tilde{F}), both corresponding to gate times t_g given in units of J^{-1} where $J = 30$ MHz. The two different values shown for \tilde{F} and $\tilde{\Omega}_{\max}$ correspond to respective high-frequency cutoffs of $\omega_0 = 500$ MHz and $\omega_0 = 450$ MHz (in brackets).

N_t	t_g [ns]	F [%]	\tilde{F} [%]	$\tilde{\Omega}_{\max}$ [MHz]
14	75.0	92.92	92.08 (91.43)	102.7 (96.0)
12	76.0	91.74	91.38 (91.20)	96.5 (96.2)
10	81.3	91.91	91.39 (91.35)	107.5 (104.7)
20	139.2	99.72	99.29 (99.28)	111.2 (112.2)
18	165.0	99.72	99.45 (99.35)	102.9 (94.9)
16	180.0	99.00	98.79 (98.77)	119.1 (116.0)
18	180.0	99.70	99.52 (99.40)	116.4 (107.2)
30	195.0	99.99	99.57 (99.15)	94.8 (83.9)
28	198.9	99.99	99.23 (98.68)	126.4 (119.0)
18	215.0	99.78	99.61 (99.59)	102.7 (100.8)
20	213.3	99.96	99.70 (99.70)	105.8 (102.0)
24	205.0	99.99	99.84 (99.72)	129.0 (122.9)
22	207.2	99.98	99.88 (99.78)	118.7 (113.4)
22	210.5	99.99	99.89 (99.86)	119.8 (114.7)
24	215.0	99.99	99.61 (99.47)	129.6 (126.9)
22	224.6	99.99	99.91 (99.79)	108.9 (101.0)
22	230.0	99.99	99.96 (99.93)	126.6 (120.4)

In reality, the fidelity loss resulting from decoherence is inextricably linked to the particular experimental setup and noise sources present in it. The errors due to decoherence certainly depend sensitively on the total gate time, which is minimized in our approach by the interplay of always-on interactions between the qubits and time-dependent control pulses acting on all qubits. Quite generally, the suppression of the gate fidelity due to decoherence is approximately given by the factor $\exp(-t_g/T_2)$, determined by the ratio of the gate time t_g and the decoherence time T_2 [9]. It is therefore quite encouraging that the required times we find for high-fidelity ($F > 90\%$) realizations of the Toffoli gate ($t_g \sim 75$ ns) represent a rather small fraction of the newly achieved decoherence times ($T_2 \sim 5 - 20 \mu\text{s}$). Remarkably, this is better than achieved experimentally (with $T_2 \sim 1 \mu\text{s}$) for two-qubit gates ($t_g \sim 30 - 60$ ns).

To summarize, employing methods of quantum operator control we have investigated the feasibility of realizing a quantum Toffoli gate with superconducting qubits in a circuit QED setup. Our calculations indicate that within 75 ns a Toffoli gate can be realized with intrinsic fidelities higher than 90%, while fidelities larger than 99% require gate times of about 140 ns. A particularly appealing feature of our approach is that it does not make a principal difference between two- and three qubit gates, in contrast to the more conventional approaches in which

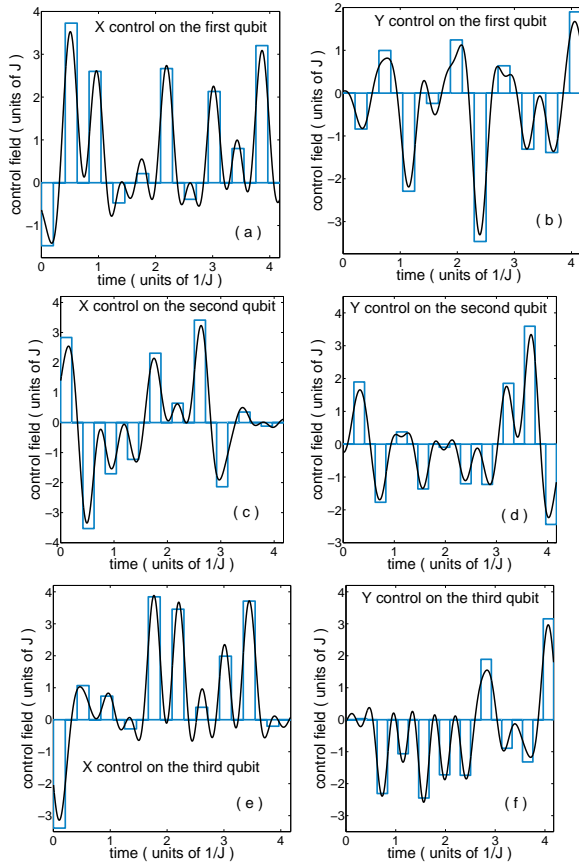


FIG. 2: Piecewise-constant and filtered ($\omega_0 = 500$ MHz) control fields acting on the three qubits for $J = 30$ MHz, i.e., a gate time t_g of $4.18J^{-1} = 139$ ns.

a Toffoli gate is realized through several two-qubit and single-qubit gates. Our method can be used for realizing other three-qubit gates (e.g., the Fredkin gate) and can also be straightforwardly generalized to an arbitrary number of qubits.

Our study can be extended using more sophisticated iterative schemes for finding optimal control pulses, and could form the basis of an open-loop type approach taking into account higher qubit levels and experimental uncertainties. The reduced gate times are likely to simplify the realization of three-qubit Toffoli gates and lead to a higher fidelity than the direct approach [13–15].

We acknowledge useful discussions with S. Aldana, S. Filipp, R. Heule, and A. Nunnenkamp. This work was financially supported by EU project SOLID, the Swiss NSF, the NCCR Nanoscience, and the NCCR Quantum Science and Technology.

- [1] For a review, see Y. Makhlin, G. Schön, and A. Shnirman, *Rev. Mod. Phys.* **73**, 357 (2001); J. Q. You and F. Nori, *Phys. Today* **58**, 42 (2005); J. Clarke and F. K. Wilhelm, *Nature (London)* **453**, 1031 (2008).
- [2] J. M. Martinis, M. H. Devoret, and J. Clarke, *Phys. Rev. Lett.* **55**, 1543 (1985).
- [3] A. Blais *et al.*, *Phys. Rev. A* **69**, 062320 (2004).
- [4] A. Wallraff *et al.*, *Nature (London)* **431**, 162 (2004).
- [5] J. Majer *et al.*, *Nature (London)* **449**, 443 (2007).
- [6] J. Koch *et al.*, *Phys. Rev. A* **76**, 042319 (2007).
- [7] Z. Kim *et al.*, *Phys. Rev. Lett.* **106**, 120501 (2011).
- [8] H. Paik *et al.*, *Phys. Rev. Lett.* **107**, 240501 (2011).
- [9] L. DiCarlo *et al.*, *Nature (London)* **460**, 240 (2009).
- [10] N. D. Mermin, *Quantum Computer Science: An Introduction* (Cambridge University Press, New York, 2007).
- [11] T. Monz *et al.*, *Phys. Rev. Lett.* **102**, 040501 (2009).
- [12] B. P. Lanyon *et al.*, *Nat. Phys.* **5**, 134 (2009).
- [13] A. Fedorov *et al.*, arXiv:1108.3966, *Nature* **481**, 170 (2012).
- [14] M. Mariantoni *et al.*, arXiv:1109.3743, *Science* **334**, 61 (2011).
- [15] M. D. Reed *et al.*, arXiv:1109.4948.
- [16] D. D'Alessandro, *Introduction to Quantum Control and Dynamics* (Taylor & Francis, Boca Raton, 2008).
- [17] S. Montangero, T. Calarco, and R. Fazio, *Phys. Rev. Lett.* **99**, 170501 (2007); M. Steffen, J. M. Martinis, and I. L. Chuang, *Phys. Rev. B* **68**, 224518 (2003); P. Rebentrost and F. K. Wilhelm, *ibid.* **79**, 060507(R) (2009); R. Fisher *et al.*, *ibid.* **81**, 085328 (2010); H. Yuan *et al.*, *Phys. Rev. A* **79**, 042309 (2009); J. M. Chow *et al.*, *ibid.* **82**, 040305 (2010).
- [18] F. Motzoi *et al.*, *Phys. Rev. Lett.* **103**, 110501 (2009).
- [19] J. M. Gambetta *et al.*, *Phys. Rev. A* **83**, 012308 (2011).
- [20] A. Galiatdinov, *Phys. Rev. A* **75**, 052303 (2007); M. R. Geller *et al.*, *ibid.* **81**, 012320 (2010); J. Ghosh and M. R. Geller, *ibid.* **81**, 052340 (2010).
- [21] J. Zhang and B. Whaley, *Phys. Rev. A* **71**, 052317 (2005).
- [22] S. G. Schirmer, I. C. H. Pullen, and P. J. Pemberton-Ross, *Phys. Rev. A* **78**, 062339 (2008); D. Burgarth *et al.*, *ibid.* **79**, 060305(R) (2009).
- [23] R. Heule *et al.*, *Phys. Rev. A* **82**, 052333 (2010); *Eur. Phys. J. D* **63**, 41 (2011).
- [24] S. Filipp *et al.*, *Phys. Rev. A* **83**, 063827 (2011).
- [25] M. Baur *et al.*, arXiv:1107.4774.
- [26] R. Fazio, G. M. Palma, and J. Siewert, *Phys. Rev. Lett.* **83**, 5385 (1999).
- [27] W. H. Press *et al.*, *Numerical Recipes in Fortran 77 and 90: The Art of Scientific and Parallel Computing* (Cambridge University Press, Cambridge, 1997).
- [28] See, e.g., S. Machnes *et al.*, *Phys. Rev. A* **84**, 022305 (2011).